I&EC research
Industrial & Engineering Chemistry Research

Article

pubs.acs.org/IECR

Effect of Cross-Link Density of the Matrix on the Damping Properties of Magnetorheological Elastomers

Yanceng Fan, Xinglong Gong,* Shouhu Xuan,* Lijun Qin, and Xiaofeng Li

CAS Key Laboratory of Mechanical Behavior and Design of Materials, Department of Modern Mechanics, University of Science and Technology of China, Hefei 230027, China

ABSTRACT: The effect of cross-link density of the matrix on the controllable damping properties of magnetorheological elastomers (MREs) has been investigated. MRE samples with different cross-link densities and plasticizer contents were fabricated and their microstructures were observed using an environmental scanning electron microscope (SEM). The dynamic performances of these samples were measured using a modified dynamic mechanical analyzer (DMA). The experimental results indicated the magneto-induced change of loss factor was enhanced by decreasing the cross-link density. The plasticizer and the frequency markedly influenced the magneto-induced change of loss factor when the cross-link density of the matrix was low. In addition, by reducing cross-link density, the magneto-induced modulus and the relative MR effect increased. A mechanism for the magneto-induced change of loss factor was proposed and the analysis implied that the rearrangement of particles is an important influence on controlling the damping properties of MREs.

1. INTRODUCTION

Magnetorheological elastomers (MREs), which are mainly composed of a polymeric matrix and soft magnetic particles, are magnetically active materials belonging to a group of smart materials.[1−14] When the constituents are well mixed in the presence of a magnetic field, the magnetic particles follow the direction of the magnetic field lines during the cross-linking process. After the curing process, the magnetic particles are fixed in their positions and form chain-like or columnar structures.[11,14] Due to the anisotropic structure and magnetic response, the rheological or mechanical properties of MREs can be changed continuously, rapidly, and reversibly when an external magnetic field is applied.[5−14]

Based on their unique characteristics, MREs have attracted increasing attention and have been considered for a wide range of applications in vibration reduction and noise reduction, etc.[4,11,15−22] Typical applications are MRE adaptive tuned vibration absorbers[15−20] and MRE isolators.[21,22] Sun et al.[19] and Hoang et al.[20] indicated that the low damping of MREs leads to high vibration reduction effect in MRE tunable vibration absorbers. For MRE-based vibration isolators, the high damping leads to a vibration reduction effect when the excitation signal is in the resonance frequency band of the system. While in the vibration isolation frequency band, the low damping leads to a high vibration reduction effect. It is noted that the performances of these MRE devices is highly dependent on their controllable damping properties (loss factor). Therefore, to develop high-efficiency MRE-based vibration reduction devices, the primary objective in this text is focused on the development of MREs with controllable damping properties.

Zhou[6] and Lokander[12] observed that the influence of magnetic field on the loss factor was small and the change of loss factor could be neglected under different applied magnetic fields. Chen et al.[23] also pointed out that the magneto-induced change of loss factor was slight. To synthesize MREs with controllable damping properties, many key issues need to be investigated. Recently, Fan et al.[24] indicated that a reduction of the binding force of the matrix exerted on the particles can increase the magneto-induced change of loss factor. Moreover, the matrix plays a key role in the controllable damping properties of MREs. By using temperature-controllable materials in the matrix, the controllability of the damping properties can be enhanced.[25] It was found that the rearrangement of particles in the matrix was one of the main influences on controlling the damping properties.[25] Under the application of a magnetic field, the movement of the particles in the cured matrix depended significantly on the resistance of the matrix. In a vulcanizable rubber, the higher cross-link density provides a stiffer matrix, which will further influence the rearrangement of particles. Therefore, the level of cross-link density of the matrix exhibited a high effect on the damping properties of MREs. To date there has been little study of the cross-link density dependent damping properties of MREs.

Consequently, this paper focuses on the effect of cross-link density on MRE damping properties. First, MRE samples with different cross-link densities were prepared by using different amounts of vulcanizing agent. Then, the microstructures of the MRE samples were observed and the influences of cross-link density, plasticizer, and frequency on the damping properties were experimentally investigated. A mechanism for the controllable damping properties was proposed and finally the effect of cross-link density on modulus and MR effect were evaluated.

2. EXPERIMENTAL DETAILS

2.1. Preparation of MREs. MRE samples mainly comprise magnetic particles in an elastic matrix. The matrix material used

Received: September 18, 2012
Revised: November 1, 2012
Accepted: December 14, 2012
Published: December 14, 2012

dx.doi.org/10.1021/ie302536e | Ind. Eng. Chem. Res. 2013, 52, 771−778

was cis-polybutadiene rubber (BR), purchased from Shanghai Gao-Qiao Petrochemical Corporation, China. The magnetic particles were carbonyl iron (type CN) purchased from BASF with an average diameter of 6 μm. The vulcanizing agent and the plasticizer were sulfur and naphthenic oil, respectively, provided by Hefei Wangyou Rubber Company of China. In this study, two groups of MRE samples were prepared: one group with different contents of vulcanizing agent (0.1, 0.5, 1, 3, and 5 phr (parts per hundred parts rubber)), and the other group with different contents of plasticizer (80, 100, 120, and 140 phr). The MRE samples had weight fractions of 60% carbonyl iron. For comparison, the reference samples were with different contents of vulcanizing agent and without any carbonyl iron.

The fabrication of MREs consists of three major steps: mixing, preforming, and curing. First, 100 phr rubber, different contents of plasticizer, different contents of vulcanizing agent, the iron particles (60 wt %) and other additives (5 phr ZnO, 1 phr stearic acid, 2 phr diaminodiphenylmethane, and 1 phr *N*-cyclohexyl-2-benzothiazolesulfenamide) were mixed homogeneously using a two-roll mill (Taihu Rubber Machinery Inc., China, model XK-160). Then for the preforming configuration, the mixture was put into a mold at 130 °C for 10 min under an external magnetic field of 1300 mT, generated by a magnet−heat couple device developed in-house.[26] Finally, the samples were vulcanized at 160 °C for 15 min under a pressure of approximately 13 MPa on a flat vulcanizer (Bolon Precision Testing Machines Co., China, model BL-6170-B). The quality characterization of the MRE samples with different contents of vulcanizing agent and 100 phr plasticizer is shown in Table 1. It

Table 1. Quality Characterization of the MRE Samples with Different Contents of Vulcanizing Agent in Which the Content of Plasticizer Was 100 phr

sulfur content (phr)	density (g/cm^3)	magnetic susceptibility (cm^3/g)	saturation magnetization (emu/g)
5	2.01	0.44	143
3	2.00	0.45	145
1	1.99	0.44	145
0.5	1.95	0.44	143
0.1	1.83	0.45	144

can be seen that the density of samples increased gradually with increases in the sulfur content, which was related to the cross-link density of the matrix. The magnetic susceptibility and saturation magnetization of samples remained almost constant with increasing sulfur content.

2.2. Magnetic Properties of Samples. To investigate the magnetic susceptibility and saturation magnetization of the samples, the magnetic properties of samples were measured by using a hysteresis measurement system (HyMDC).

2.3. Testing of Cross-Link Density. The cross-link densities of samples were tested by using a nuclear magnetic resonance cross-link density meter (MicroMR-CL), provided by Shanghai Niumai Electronic Technology Co., China. All operations were performed at a magnetic field of 520 mT, a frequency of 21.8 MHz, and constant temperature of 35 °C.

2.4. Observation of Microstructure. The microstructures of samples were observed by using an environmental scanning electron microscope (SEM; Philips of Holland, model XL-30 ESEM). Each sample was cut into flakes and coated with a thin layer of gold prior to the SEM observation. The microstructure of samples was observed at an accelerating voltage of 20 kV.

2.5. Measurement of Dynamic Properties. Dynamic mechanical properties of samples were measured by using a modified dynamic mechanical analyzer (DMA).[26] In this system, a self-made electromagnet was introduced to generate a variable magnetic field from 0 to 1000 mT, which was attached to a conventional DMA (Triton Technology Ltd., UK, model Tritec 2000B).

In the experiments, the MRE samples had dimensions of 10 mm × 10 mm × 3 mm, and the particle chains were parallel with the thickness direction of sample (Figure 1). Both

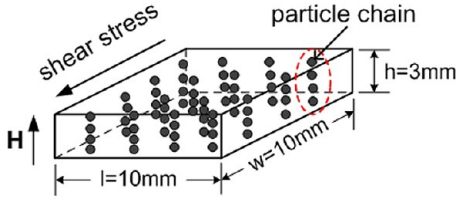

Figure 1. Sketch of the structure of tested MRE samples, in which H is the testing magnetic field.

magnetic field sweep testing (field range 0−1000 mT) and frequency sweep testing (frequency range 1−30 Hz) were conducted to measure dynamic properties, such as shear storage modulus and loss factor. The shear strain amplitude was set at 0.3%. The magnetic field and the shear stress were parallel and perpendicular with the direction of the particle chains, respectively (Figure 1). The experiments were carried out at room temperature.

3. RESULTS AND DISCUSSION

In this study, samples with different contents of vulcanizing agent (sulfur) were prepared. Figure 2 shows the cross-link density and storage modulus of samples with different contents of sulfur. The tests of storage modulus were conducted at a frequency of 10 Hz, constant shear strain amplitude of 0.3%, and constant magnetic field of 0 mT. The cross-link density is defined as cross-links content per unit volume. It can be seen that the cross-link density increased gradually with increases in sulfur content. The storage modulus has a positive relationship with the cross-links.[27,28] Therefore, the storage modulus of samples was increased by increasing the sulfur content. Here, the effects of cross-link density of the matrix on the loss factor and other dynamic properties were also investigated.

3.1. Loss Factor. *3.1.1. Effect of Vulcanizing Agent on the Loss Factor.* For the samples prepared with various contents of sulfur, the loss factors under different magnetic fields from 0 to 1000 mT are shown in Figure 3, where a and b correspond to the reference samples and the MRE samples, respectively. For all these samples, the content of the plasticizer was 100 phr. It can be seen that the loss factor of samples decreased gradually with increases in sulfur content. The increased cross-links reduced the movement of molecular chains and the energy dissipation of samples decreased. Moreover, under increasing magnetic field strength, the loss factor of the MRE samples showed a decreasing trend. With increases in sulfur content, the magneto-induced change of loss factor of the MRE samples decreased gradually. For the reference samples, the loss factor exhibited no change for the full range of magnetic fields. This is to be expected as there were no particles to induce the change of loss factor.

dx.doi.org/10.1021/ie302536e | *Ind. Eng. Chem. Res.* 2013, 52, 771−778

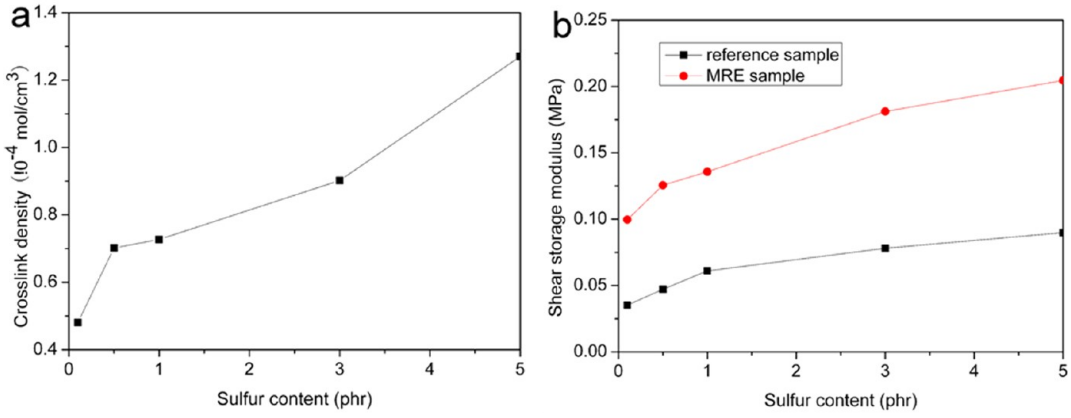

Figure 2. Cross-link density and shear storage modulus of samples with different contents of sulfur.

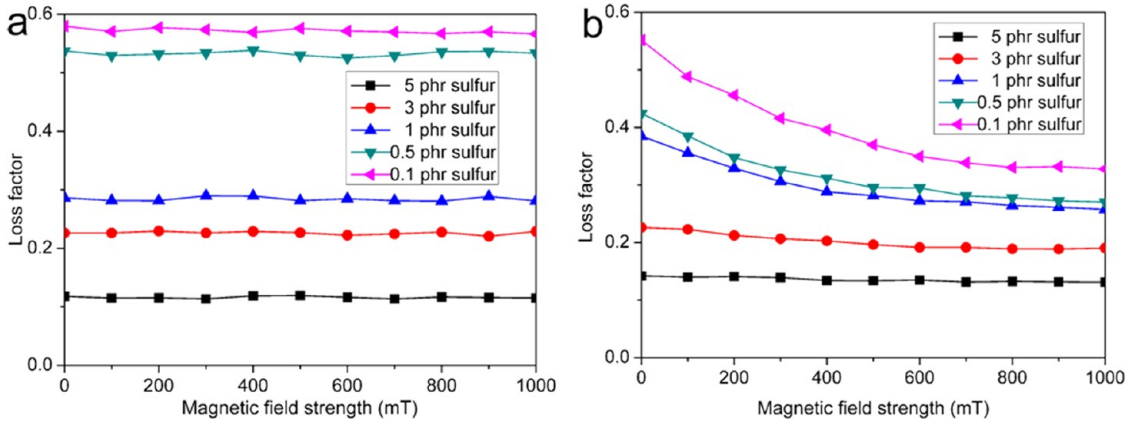

Figure 3. Magnetic field strength dependency of the loss factor of samples with various contents of sulfur: (a) reference samples; (b) MRE samples. The tests were conducted at a frequency of 10 Hz.

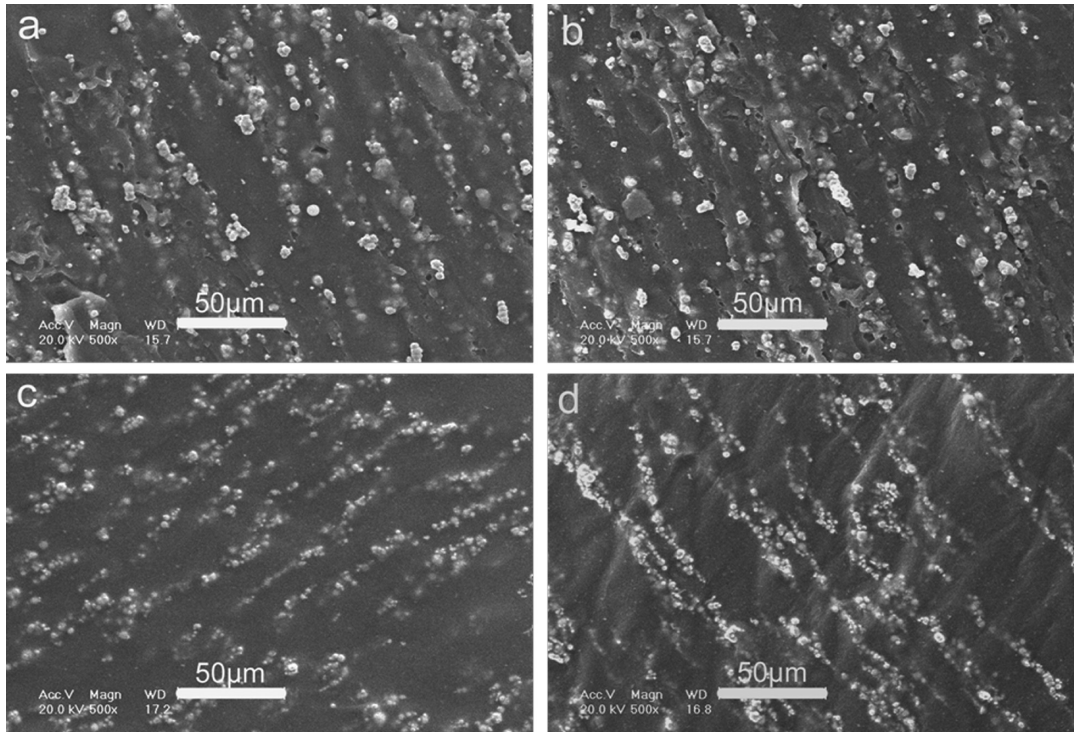

Figure 4. SEM images of the MRE samples: (a) and (b) samples with 5 phr sulfur; (c) and (d) samples with 0.1 phr sulfur. The micrographs (b) and (d) depict samples where an additional magnetic field was applied.

dx.doi.org/10.1021/ie302536e | *Ind. Eng. Chem. Res.* 2013, 52, 771−778

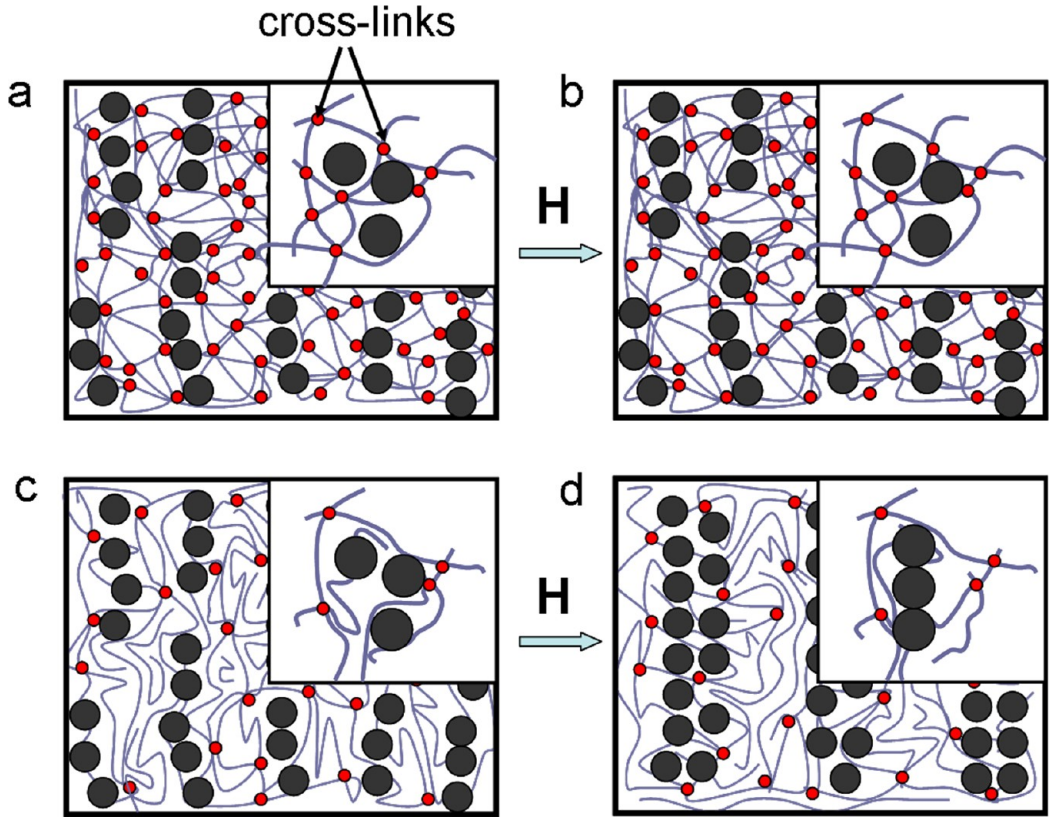

Figure 5. Sketch of the microscopic structures of samples with different contents of sulfur: (a) and (b) the microscopic structures of sample with 5 phr sulfur; (c) and (d) the microscopic structures of sample with 0.1 phr sulfur. When an additional magnetic field was applied to (a) and (c), the microscopic structures correspond to (b) and (d), respectively.

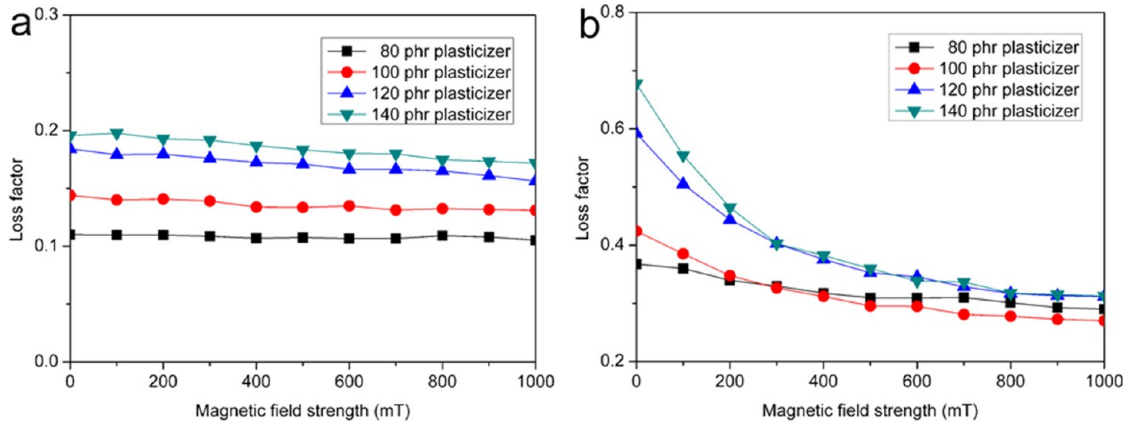

Figure 6. Loss factor of samples with various contents of plasticizer under different magnetic fields: (a) and (b) correspond to the samples with 5 phr sulfur and 0.5 phr sulfur, respectively. The frequency was set at 10 Hz for all tests.

3.1.2. Mechanism. To understand the performance of the magneto-induced change of loss factor of the MRE samples with different contents of sulfur, the microstructures of the MRE samples were observed and a mechanism was proposed.

Some of the SEM micrographs of the MRE samples are shown in Figure 4, where parts a and b correspond to the samples with 5 phr sulfur, and parts c and d correspond to the samples with 0.1 phr sulfur. During the preforming process, the bulk samples were exposed to an external magnetic field of 1300 mT for 10 min. The particle chain structures, which were parallel to the direction of the external magnetic field, were formed in the matrix (Figure 4) and the final MRE composite was obtained. Because the samples were vulcanized under pressure, the particle chain structures were not perfect (Figure 4a and 4c). To investigate the stability of the particle chain structures, an additional magnetic field (500 mT), parallel to the direction of the particle chains, was further applied to the samples a and c for 20 min prior to the SEM observation (Figure 4b and 4d). For the samples with 5 phr sulfur, almost no change of the particle chain structure in the matrix was observed before and after applying the additional magnetic field. In comparison, Figure 4c and 4d indicate that the particle chain structures became longer and thicker when the external magnetic field was applied for the sample with 0.1 phr sulfur (Figure 4d).

dx.doi.org/10.1021/ie302536e | *Ind. Eng. Chem. Res.* 2013, 52, 771−778

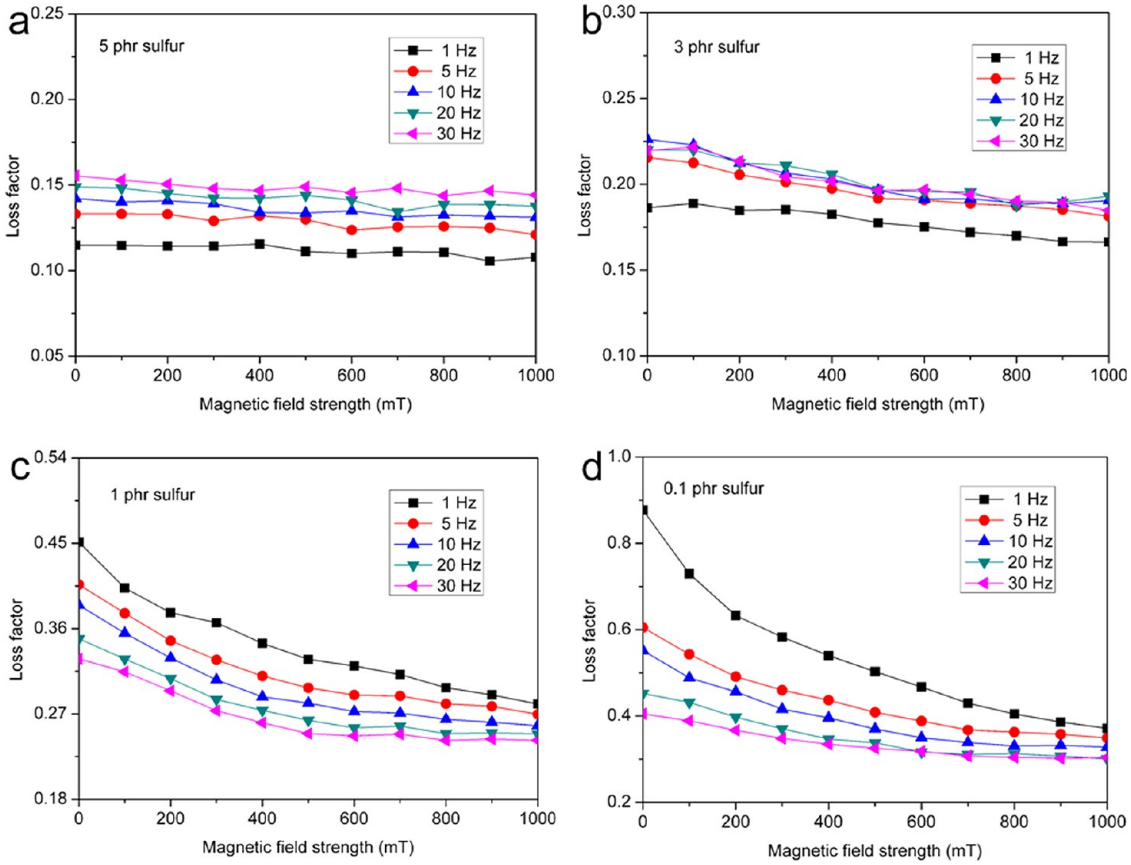

Figure 7. Magnetic field strength dependency of the loss factor of samples with different contents of sulfur under different frequencies.

Figure 5 shows the microscopic structures of samples with different contents of sulfur diagrammatically, in which parts a and b correspond to the microscopic structures of sample with 5 phr sulfur, and parts c and d correspond to the microscopic structures of sample with 0.1 phr sulfur. When an additional magnetic field was applied to the samples a and c, the microscopic structures transformed to b and d, respectively. The cross-link density of sample with 5 phr sulfur was higher than that of sample with 0.1 phr sulfur. It is well-known that the more cross-links can result in a stronger binding force. Due to the high binding force of the matrix, the particles in the sample with 5 phr sulfur were unmovable even when the magnetic field was applied (Figures 4b and 5b). When the content of sulfur was reduced, the cross-links of the matrix were reduced and the movement of the matrix molecular chains increased. Therefore, the particle chains can form improved chain structures under an applied magnetic field due to a weak binding force (Figures 4d and 5d). The interaction between the particles will be strengthened by forming improved chain structures. In this case, the effect of particle obstruction was enhanced when the magnetic field strength increased and the friction between the matrix molecular chains was reduced. Therefore, with decreasing sulfur content, there is a clear decrease in the trend for loss factor and the reduction in loss factor increased gradually under different magnetic fields as sulfur content decreased (Figure 3b).

3.1.3. Effect of Plasticizer and Frequency on the Loss Factor. Here, the effect of plasticizer on the loss factor of samples under different magnetic fields was investigated (Figure 6). Parts a and b correspond to the samples with 5 and 0.5 phr sulfur, respectively. As the plasticizer content increased, the loss factor of samples increased gradually. The friction between the matrix molecular chains, between the matrix and the particles, and also between the particles increased for the increased plasticizer content. It is also interesting to see that the magneto-induced change of loss factor of sample with 0.5 phr sulfur exhibited an increasing trend with heightening levels of plasticizer, which increased from 0.08 (80 phr plasticizer) to 0.36 (140 phr plasticizer). However, the effect of plasticizer on the magneto-induced change of loss factor of sample with 5 phr sulfur was slight. The interaction between the matrix molecular chains was reduced by adding the plasticizer. The reduced interaction can increase the movement of molecular chains and improved chain structures can be formed under the applied magnetic field. For the low cross-link density matrix, there were more mobile molecular chains than for the high cross-link density matrix. Thus, with increases in plasticizer content, the magneto-induced change of loss factor of sample with 0.5 phr sulfur increased gradually for enhanced chain structures.

In Figure 7, the effect of frequency on the loss factor of samples with different cross-link densities is shown for a content of plasticizer of 100 phr. With increasing of the frequency, the loss factors displayed different tendencies: an increasing trend for the sample with 5 phr sulfur, but a decreasing trend for the samples with 1 and 0.1 phr sulfur, and a tendency of increased plus decreased loss factor for the sample with 3 phr sulfur. These different tendencies of the loss factor were attributed to the different cross-link densities of the matrix, which can lead to different sizes of motion units of molecular chains under a shear force. Different sizes of motion units own various relaxation times. The relaxation time τ can be expressed as

dx.doi.org/10.1021/ie302536e | *Ind. Eng. Chem. Res.* 2013, 52, 771−778

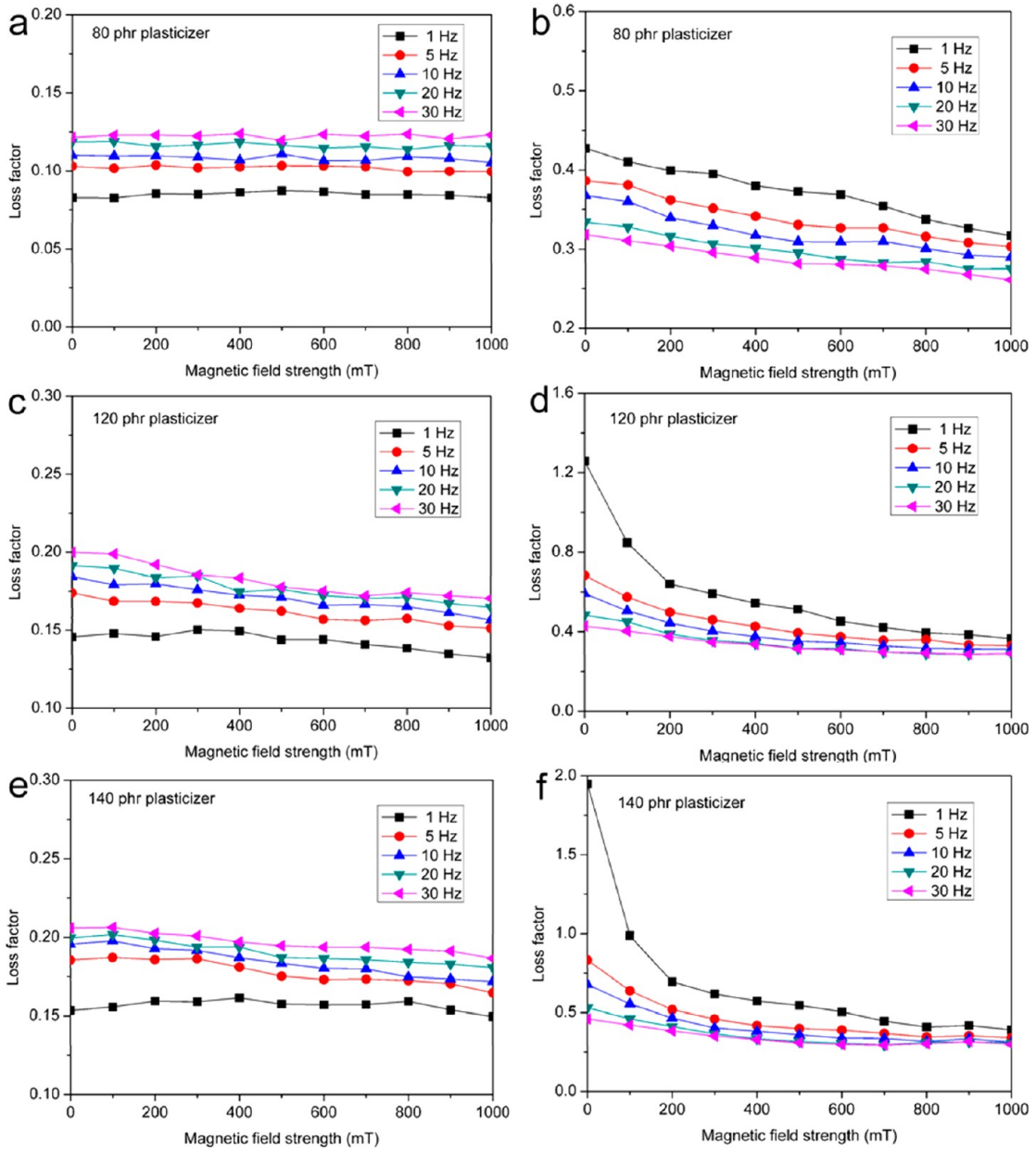

Figure 8. Magnetic field strength dependency of the loss factor of samples with different contents of plasticizer under different frequencies: (a), (c), and (e) correspond to the samples with 5 phr sulfur; (b), (d), and (f) correspond to the samples with 0.5 phr sulfur.

$$\tau = \tau_0 e^{(\Delta H - \gamma\sigma)/RT} \quad (1)$$

where ΔH, σ, γ, T, R, and τ_0 are the activation energy of molecular chains, stress, proportionality coefficient, temperature, gas constant, and constant, respectively. Under the same environment, the small motion units led to low activation energy and the relaxation time was short. When the cross-link density of the matrix was high, the relaxation time of molecular chains was short. With increasing of the frequency, the molecular chains could catch up with the shear frequency and the friction between the molecular chains increased until the molecular chains became entangled. Thus, the loss factor of sample with 5 phr sulfur increased with increasing frequency (Figure 7a). When the cross-link density of the matrix decreased, the number of mobile molecular chains increased and the relaxation time of molecular chains was long. With increasing of the frequency, more and more mobile molecular chains could not catch up with the shear frequency for the long relaxation time and the number of tangled molecular chains increased. The tangling of molecular chains reduced friction between these chains. So the loss factor of samples with 1 and 0.1 phr sulfur decreased with increasing frequency (Figure 7c and 7d). For the samples with different cross-link densities, the magneto-induced changes of loss factor under different frequencies were varied. The particles in the matrix were almost unmovable under the applied magnetic field when the cross-link density was high (Figure 5b). Thus, the magneto-induced change of loss factor was slight under different frequencies (Figure 7a and 7b). When the cross-link density of the matrix was low, the increased frequency could lead to increment of the tangled molecular chains. In this case, the movement of the particles was decreased and the effect of particle obstruction was reduced. Therefore, for a sample with a low cross-link density matrix, the magneto-induced change of

dx.doi.org/10.1021/ie302536e | Ind. Eng. Chem. Res. 2013, 52, 771−778

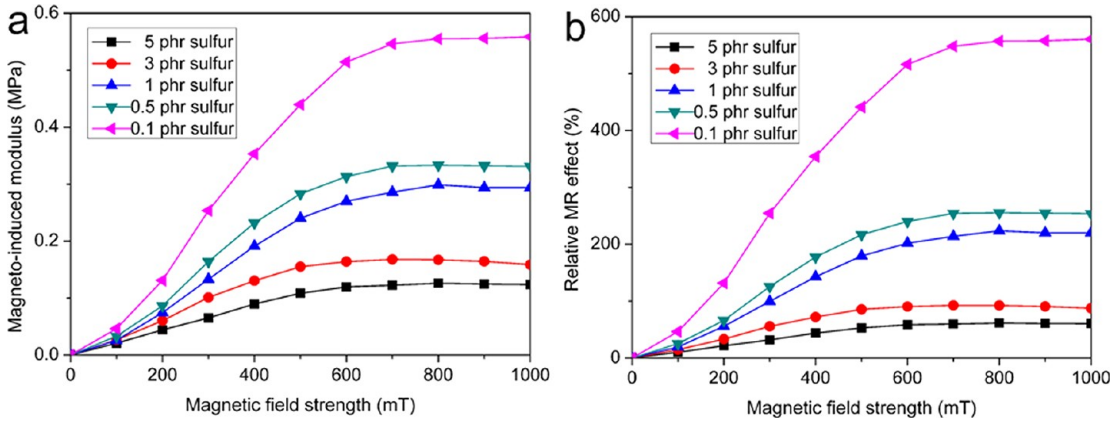

Figure 9. Magnetic field strength dependency of the magneto-induced modulus and relative MR effect of samples with various contents of sulfur. The tests were conducted at a frequency of 10 Hz.

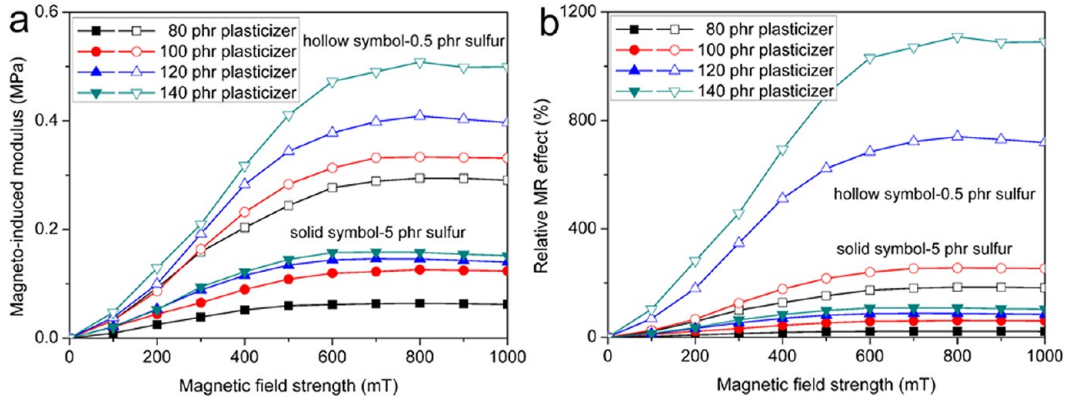

Figure 10. Magnetic field strength dependency of magneto-induced modulus and relative MR effect of samples with various contents of plasticizer. The frequency was set at 10 Hz.

loss factor decreased gradually with increasing frequency (Figure 7c and 7d).

Under different frequencies, the effect of plasticizer on the loss factor of samples with different cross-link densities is shown in Figure 8. Parts a, c, and e correspond to the samples with 5 phr sulfur. As can be seen, the magneto-induced change of loss factor was slight for different plasticizer contents. While for the samples with 0.5 phr sulfur, the magneto-induced change of loss factor exhibited obvious differences under different contents of plasticizer (Figure 8b, 8d, and 8f). With increasing levels of plasticizer, the magneto-induced change of loss factor clearly increased at low frequency. The reason for this is that the number of tangled molecular chains was small at low frequency and the reduced friction between the tangled chains was little. So the friction between the molecular chains is large for the existence of much mobile molecular chains. Under a magnetic field, the effect of particle obstruction was obvious. Especially at 1 Hz, the magneto-induced change of loss factor increased from 0.11 (80 phr plasticizer) to 1.56 (140 phr plasticizer). The plasticizer not only increased the friction but also increased the movement of molecular chains. Thus, with increasing levels of plasticizer, the magneto-induced change of loss factor of samples with 0.5 phr sulfur clearly increased at low frequency. When the frequency increased, the number of tangled molecular chains increased. The friction between the molecular chains reduced and the effect of particle obstruction decreased for different magnetic fields.

3.2. Magneto-Induced Modulus and MR Effect. For the MRE samples with different cross-link densities, the magneto-induced modulus and relative MR effect under different magnetic fields were also evaluated, as shown in Figure 9, in which the content of plasticizer was 100 phr. The magneto-induced modulus and the relative MR effect are defined as $\Delta G = G' - G'_0$ and $\mathrm{RMe}(\%) = \Delta G/G'_0$, respectively. G'_0 is the initial storage modulus and G' is the storage modulus for different applied magnetic fields. As shown in Figure 9, the magneto-induced modulus and the relative MR effect showed an increasing trend with magnetic field increases before they reach magnetic saturation for high magnetic fields and this phenomenon is similar to that observed in our previous work.[24,29] Obviously, the magneto-induced modulus and the relative MR effect decreased with increasing of the cross-link density. In a low cross-link density matrix, the movement of particles increased and improved particle chain structures were formed under the applied magnetic fields. Thus, the effect of the particle obstruction was enhanced and the storage modulus was also increased. Under an applied magnetic field, the enhanced particle chain structures can be formed more easily in the matrices with low cross-link density. Therefore, the particle chain structures in the matrix play a key role in the magneto-induced modulus and the relative MR effect.

The effect of plasticizer on magneto-induced modulus and relative MR effect were investigated (Figure 10). With increasing plasticizer content, the magneto-induced modulus and the relative MR effect increased gradually. The plasticizer

dx.doi.org/10.1021/ie302536e | Ind. Eng. Chem. Res. 2013, 52, 771−778

reduced the interaction between the molecular chains, thus under the preforming process, the particles moved more easily when the content of plasticizer was high, which further led to the higher magneto-induced modulus and the greater relative MR effect. For the samples with 5 and 0.5 phr sulfur, the increased amplitude of the magneto-induced modulus was different. The rearrangement of particles in the low cross-link density matrix was the main reason, which was also the reason for the increased MR effect. This further suggests that the rearrangement of particles in the matrix can markedly reinforce the magneto-induced modulus and the relative MR effect.

4. CONCLUSION

This work focused on the influence of the cross-link densities of the matrix on the controllable damping properties of MRE samples. The microstructural observations indicated that the magnetic particles can rearrange in low cross-link density matrices. Under different magnetic fields, the effects of cross-link density, plasticizer, and frequency on the loss factor and other dynamic properties were experimentally investigated. The magneto-induced change of loss factor was enhanced by decreasing the cross-link density. For the MRE samples with low cross-link density, the effect of plasticizer and frequency on the magneto-induced change of loss factor was clearly observed. Moreover, the magneto-induced modulus and the relative MR effect were also increased by decreasing the cross-link density. The reduced cross-link density of the matrix increased the movement of magnetic particles and consequently a mechanism for controllable damping properties was proposed. The analysis indicated that the rearrangement of particles plays an important role in the enhanced magneto-induced change of loss factor, magneto-induced modulus, and relative MR effect. These results could be useful in future investigations of the controllability of MRE damping properties.

AUTHOR INFORMATION

Corresponding Author

*E-mail: gongxl@ustc.edu.cn (X.G.) and xuansh@ustc.edu.cn (S.X.).

Notes

The authors declare no competing financial interest.

ACKNOWLEDGMENTS

Financial supports from the National Natural Science Foundation of China (Grants 11125210, 11072234, 11102202), the National Basic Research Program of China (973 Program, Grant 2012CB937500), and the Specialized Research Fund for the Doctoral Program of Higher Education of China (Project 20093402110010) are gratefully acknowledged.

REFERENCES

(1) Shiga, T.; Okada, A.; Kurauchi, T. Magnetroviscoelastic behavior of composite gels. *J. Appl. Polym. Sci.* **1995**, *58*, 787.
(2) Jolly, M. R.; Carlson, J. D.; Muñoz, B. C. A model of the behaviour of magnetorheological materials. *Smart Mater. Struct.* **1996**, *5*, 607.
(3) Farshad, M.; Le Roux, M. Compression properties of magnetostrictive polymer composite gels. *Polym. Test.* **2005**, *24*, 163.
(4) Carlson, J. D.; Jolly, M. R. MR fluid foam and elastomer devices. *Mechatronics* **2000**, *10*, 555.
(5) Bellan, C.; Bossis, G. Field dependence of viscoelastic properties of MR elastomers. *Int. J. Mod. Phys. B* **2002**, *16*, 2447.
(6) Zhou, G. Y. Shear properties of a magnetorheological elastomer. *Smart Mater. Struct.* **2003**, *12*, 139.
(7) Li, W. H.; Zhou, Y.; Tian, T. F. Viscoelastic properties of MR elastomers under harmonic loading. *Rheol. Acta* **2010**, *49*, 733.
(8) Guan, X. C.; Dong, X. F.; Ou, J. P. Magnetostrictive effect of magnetorheological elastomer. *J. Magn. Magn. Mater.* **2008**, *320*, 158.
(9) Gong, X. L.; Zhang, X. Z.; Zhang, P. Q. Fabrication and characterization of isotropic magnetorheological elastomers. *Polym. Test.* **2005**, *24*, 669.
(10) Zhou, G. Y.; Li, J. R. Dynamic behavior of a magnetorheological elastomer under uniaxial deformation: I. Experiment. *Smart Mater. Struct.* **2003**, *12*, 859.
(11) Ginder, J. M.; Nichols, M. E.; Elie, L. D.; Tardiff, J. L. Magnetorheological elastomers: Properties and applications. *Proc. SPIE* **1999**, *3675*, 131.
(12) Lokander, M.; Stenberg, B. Improving the magnetorheological effect in isotropic magnetorheological rubber materials. *Polym. Test.* **2003**, *22*, 677.
(13) Li, W. H.; Zhang, X. Z. A study of the magnetorheological effect of bimodal particle based magnetorheological elastomers. *Smart Mater. Struct.* **2010**, *19*, 035002.
(14) Zhang, W.; Gong, X. L.; Xuan, S. H.; Xu, Y. G. High-performance hybrid magnetorheological materials: Preparation and mechanical properties. *Ind. Eng. Chem. Res.* **2010**, *49*, 12471.
(15) Ginder, J. M.; Schlotter, W. F.; Nichols, M. E. Magneto-rheological elastomers in tunable vibration absorbers. *Proc. SPIE* **2001**, *4331*, 103.
(16) Albanese, A. M.; Cunefare, K. A. Properties of a magneto-rheological semiactive vibration absorber. *Proc. SPIE* **2003**, *5052*, 36.
(17) Deng, H. X.; Gong, X. L.; Wang, L. H. Development of an adaptive tuned vibration absorber with magnetorheological elastomer. *Smart Mater. Struct.* **2006**, *15*, N111.
(18) Lerner, A. A.; Cunefare, K. A. Performance of MRE-based vibration absorbers. *J. Intell. Mater. Syst. Struct.* **2008**, *19*, 551.
(19) Sun, H. L.; Zhang, P. Q.; Gong, X. L.; Chen, H. B. A novel kind of active resonator absorber and the simulation on its control effort. *J. Sound. Vib.* **2007**, *300*, 117.
(20) Hoang, N.; Zhang, N.; Du, H. A dynamic absorber with a soft magnetorheological elastomer for powertrain vibration suppression. *Smart Mater. Struct.* **2009**, *18*, 074009.
(21) York, D.; Wang, X. J.; Gordaninejad, F. A new MR fluid-elastomer vibration isolator. *J. Intell. Mater. Syst. Struct.* **2007**, *18*, 1221.
(22) Blom, P.; Kari, L. Smart audio frequency energy flow control by magneto-sensitive rubber isolators. *Smart Mater. Struct.* **2008**, *17*, 015043.
(23) Chen, L.; Gong, X. L.; Li, W. H. Effect of carbon black on the mechanical performances of magnetorheological elastomers. *Polym. Test.* **2008**, *27*, 340.
(24) Fan, Y. C.; Gong, X. L.; Jiang, W. Q.; Zhang, W.; Wei, B.; Li, W. H. Effect of maleic anhydride on the damping property of magnetorheological elastomers. *Smart Mater. Struct.* **2010**, *19*, 055015.
(25) Gong, X. L.; Fan, Y. C.; Xuan, S. H.; Xu, Y. G.; Peng, C. Control of the damping properties of magnetorheological elastomers by using polycaprolactone as a temperature-controlling component. *Ind. Eng. Chem. Res.* **2012**, *51*, 6395.
(26) Chen, L.; Gong, X. L.; Jiang, W. Q.; Yao, J. J.; Deng, H. X.; Li, W. H. Investigation on magnetorheological elastomers based on natural rubber. *J. Mater. Sci.* **2007**, *42*, 5483.
(27) Bandyopadhyay, A.; Valavala, P. K.; Clancy, T. C.; Wise, K. E.; Odegard, G. M. Molecular modeling of crosslinked epoxy polymers: The effect of crosslink density on thermomechanical properties. *Polymer* **2011**, *52*, 2445.
(28) Bengtsson, M.; Oksman, K. The use of silane technology in crosslinking polyethylene/wood flour composites. *Composites: Part A* **2006**, *37*, 752.
(29) Gong, X. L.; Chen, L.; Li, J. F. Study of utilizable magnetorheological elastomers. *Int. J. Mod. Phys. B* **2007**, *21*, 4875.